Functional Interactions Between the Subunits of the Lactose Transporter from *Streptococcus thermophilus*

Eric R. Geertsma, Ria H. Duurkens and Bert Poolman

Abstract

Although the quaternary state has been assessed in detail for only a few members of the major facilitator superfamily (MFS), it is clear that multiple oligomeric states are represented within the MFS. One of its members, the lactose transporter LacS from *Streptococcus thermophilus* assumes a dimeric structure in the membrane and *in vitro* analysis showed functional interactions between both subunits when proton motive force (Δp)-driven transport was assayed. To study the interactions in further detail, a covalent dimer was constructed consisting of *in tandem* fused LacS subunits. These covalent dimers, composed of active and completely inactive subunits, were expressed in *Escherichia coli*, and initial rates of Δp-driven lactose uptake and lactose counterflow were determined. We now show that also *in vivo* both subunits functionally interact, that is, partial complementation of the inactive subunit was observed for both transport modes. Thus, both subunits not only functionally interact in Δp-driven uptake but also in counterflow transport. In addition, analysis of in tandem fused LacS subunits containing one regulatory LacS-IIA domain showed that regulation is primarily an intramolecular event.

Introduction

The Major Facilitator Superfamily (MFS) forms the largest family of secondary transporters. Its members, found in all living organisms, catalyze the translocation of a variety of substrates among which are sugars, peptides, anions, cations and hydrophobic compounds. Most MFS proteins consist of 12 α-helical transmembrane spanning segments (TMS) that are connected by loop regions ranging from a few amino acids to several dozens of residues (75). Although data on functional and structural aspects of these proteins are produced at great pace, information on the quaternary state(s) is scarce. For both the lactose transporter LacY (99) and the sugar-phosphate antiporter UhpT (4) from *E. coli*, the monomeric unit is sufficient for transport, and earlier claims for LacY dimers are thought to be based on improper experimentation and inaccurate data interpretation. For the anion exchanger AE1 (17,111) and glucose transporter GluT1 (140) from human, and the tetracycline transporter TetA (50,136) from *E. coli*, on the other hand, there is compelling evidence that these transporters form higher oligomeric structures, and functional interactions between the subunits of the oligomers have been shown.

For secondary transporters outside the MFS, oligomeric states higher than the monomer have also been proposed (e.g., the Na^+/H^+ antiporter NhaA (37) and the multidrug exporter AcrB (72) from *E. coli*, the Na^+/glycine betaine symporter BetP (139) from *Corynebacterium glutamicum*, and the human glial glutamate transporter hEAAT2 (36); for a recent review see

(123)). For most of these transporters, it remains to be determined whether functional interactions between subunits take place. Furthermore, in those cases where cooperativity between subunits has been shown, the role of the oligomeric structure in the mechanism of transport is still far from clear.
Members of the galactoside-pentoside-hexuronide transporter family (GPH-family) of the MFS (101) are of pro- or eukaryotic origin and catalyze the transport of sugars and sugar derivatives in symport with cations (84,93). These transporters consist of twelve α-helical transmembrane segments that span the membrane in a zig-zag fashion. Detailed analysis of the oligomeric state has only been conducted for the lactose transporter LacS from *Streptococcus thermophilus* and this system forms a structural and functional dimer. For the xyloside transporter XylP from *Lactobacillus pentosus* a dimeric structure has also been reported. On the other hand, the projection structure of another GPH-family member, the melibiose permease MelB from *E. coli*, does not comply with a dimeric state (45).
Both XylP and LacS have been analyzed in the detergent-solubilized state using blue native gel electrophoresis and analytical ultracentrifugation and shown to be in a dynamic monomer to dimer equilibrium (32,123). The extent of dimerization could be manipulated by varying the detergent type or concentration. The membrane-embedded oligomeric state of XylP and LacS has been determined using freeze-fracture electron microscopy, which suggested that both proteins are present in the bilayer as dimers only (32,123). Additional evidence for this dimeric state of LacS in the membrane came from saturation-transfer electron spin resonance (109). Chemical cross-linking of cysteine substitution mutants of LacS *in situ* suggested that on the extracellular side of LacS, TMS V and VIII, and on the cytoplasmic side TMS VI and VII, are located near the centre of the LacS dimer (35). By studying LacS heterodimers of active [LacS(C320A)] and (conditionally) inactive [LacS(E67C/C320A)] species in proteoliposomes, it has been shown that the subunits within the dimer cooperate (124). Cooperativity was observed during lactose accumulation driven by the proton motive force (Δp), but not for the lactose exchange mode of transport.
Within a LacS subunit, two domains can be discerned. The N-terminal membrane-embedded carrier domain catalyzes the translocation event. The C-terminal hydrophilic LacS-IIA domain, unique for the LacS-subfamily within the GPH-family (84), is homologous to IIA^{Glc} domains of the PEP-phosphotransferase system and resides at the cytoplasmic face of the membrane. The LacS-IIA domain is not essential for transport, but serves a regulatory role. Phosphorylation of LacS-IIA by HPr(His~P) enables the domain to interact with the carrier domain and modulate the transport activity (chapter 3 and (41,83)).
In order to increase our insights into the functional role(s) of the subunit interactions, heterodimers were formed by fusing two different LacS carrier domains *in tandem*. In whole *E. coli* cells, functional interactions between a LacS(D71C/C320A) subunit, which is inactive in all modes of transport but still adopts a conformation capable of substrate-binding (122), and the active LacS(C320A) subunit were analyzed. In addition, the regulation of the LacS-carrier domain by LacS-IIA was studied in an asymmetric covalent dimer, in which only one subunit was equipped with a LacS-IIA domain.

Materials and Methods

Bacterial strains

E. coli JM110 (27,134) was used for intermediate cloning steps. The final constructs were expressed in *E. coli* MC1061 (relevant genotype: Δ*lac*ZY, *ara*BADC$^-$) (130). Both strains were cultivated at 37°C on Luria Broth under vigorous aeration. When appropriate the medium was supplemented with 50 μg/ml ampicillin.

Plasmid constructions

DNA manipulations were done according to standard protocols. The construction of pBADlacSC320A, pSKE8EhisC320A-BamH1-IIA, pNlacSC320Ahis and pSKlacSC320AΔIIA have been described in chapter 3. Plasmids pSKE8EhisC320A and pSKE8EhisC320A/D71C were described previously (122).

pSKlacSC320A/D71CΔIIA – The *NcoI-XhoI* fragment of pSKlacSC320AΔIIA was replaced by the 2147 bp *NcoI-XhoI* fragment from pSKE8EhisC320A/D71C.

pBADlacSΔIIAlacSΔIIA – In order to incorporate the D71C mutation in the first subunit, the 200 bp *AatII-NcoI* fragment from pSKE8EhisC320A-BamH1-IIA was replaced by the *AatII-NcoI* fragment from pSKE8EhisC320A/D71C, yielding pSKE8EhisC320A/D71C-BamH1-IIA. Plasmid pSKE8EhisC320A(/D71C)-BamH1-IIA was *BamH1-SpeI* digested and ligated to a linker of two annealed oligonucleotides (linkerBS and linkerSB; see Table 1) with extensions resembling a *BamH1*- or a *SpeI*-overhang. The *AatII-XbaI* fragment of this product was ligated into *AatII-XbaI* digested pBADlacSC320A, yielding pBADsub1C320A(/D71C). In order to construct the plasmid containing the second subunit, pNlacSC320Ahis was digested with *BclI-NcoI* and the 389 bp fragment was replaced by a linker of two annealed oligonucleotides (linkerBN and linkerNB; see Table 1) with extensions resembling a *BclI*- or a *NcoI*-overhang, yielding pBADsub2C320A+IIA. The sequence coding for the LacS-IIA-domain was removed by exchange of the 2229 bp *AatII-XbaI* fragment for the 1723 bp *AatII-XbaI* fragment from pSKlacSC320A(/D71C)ΔIIA, producing pBADsub2C320A(/D71C)ΔIIA. To link both subunits, the 34bp *BclI-XbaI* fragment from pBADsub1C320A(/D71C) was exchanged for the 2333 bp *BclI-XbaI* fragment from pBADsub2C320A(/D71C)ΔIIA containing the second subunit, yielding pBADlacSΔIIAlacSΔIIA. Four derivatives of pBADlacSΔIIAlacSΔIIA were generated, containing the D71C mutation in the first, the last, or both subunits.

pBADlacSΔIIAlacS+IIA – The construction of the vector harbouring a gene coding for a fusion between a LacS carrier domain and full length LacS was similar to the construction of the vector for two fused LacS carrier domains. Instead of pBADsub2C320A(/D71C)ΔIIA, plasmid pBADsub2C320A(/D71C)+IIA was used. The D71C mutation was added by exchanging the 2229 bp *AatII-XbaI* fragment of pBADsub2C320A+IIA for the 2229 bp *AatII-XbaI* fragment of pSKE8EhisC320A/D71C.

Table 1. **The complementary oligonucleotides constituting parts of the linker connecting both LacS-carrier domains.** LinkerBS and LinkerSB constitute a double stranded linker with artificial *BamHI* and *SpeI* overhangs. LinkerBN and LinkerNB constitute a double stranded linker with artificial *BclI* and *NcoI* overhangs. The sequence of both double-stranded linkers partially overlaps; double stranded linkers were created by mixing both oligonucleotides in equal ratios, boiling for 5 minutes and annealing by slowly cooling down to room temperature.

Primer	Sequence
LinkerBS	5′gatccggtgatcaggagaacctctattttcaaggca
LinkerSB	5′ctagtgccttgaaaatagaggttctcctgatcaccg
LinkerBN	5′gatcaggagaacctctattttcaaggcactagtgc
LinkerNB	5′catggcactagtgccttgaaaatagaggttctcct

Whole cell transport assays

Cultivation – *E. coli* MC1061 cells were cultivated, washed and concentrated as described in chapter 3. Cultures were induced with 1 x 10^{-3}% and 2 x 10^{-3}% (wt/vol) L-arabinose when LacS derivatives or LacS-LacS fusion proteins were expressed, respectively. Cells used for lactose exchange transport were induced with 1.5 x 10^{-4}% (wt/vol) L-arabinose when LacS or LacSΔIIA were expressed. Concentrated cell preparations were kept on ice until lactose transport was assayed.

Transport assays – General handlings involved in lactose transport in *E. coli* MC1061 cells and the preparation of cells to be used for proton motive force (Δp)-driven lactose uptake and lactose counterflow transport have been described in chapter 3.
Lactose exchange transport – Cells were concentrated to 45 mg protein/ml and incubated overnight in 50 mM KPi, pH 7.7, 2 mM $MgSO_4$ (KPM) plus 5 mM ^{14}C-lactose. The next day, cells were de-energized by incubation with the protonophore SF6847 (50 μM) plus 30 mM NaN_3 for 2 hours. Lactose exchange was assayed at 20°C by 100-fold dilution of the cells into KPM pH 7.7, supplemented with 50 μM SF6847. The external lactose concentration varied from 50 μM to 20 mM.

Membrane vesicle isolation

Inside-out membrane vesicles from *E. coli* MC1061 cells were prepared as described (35). Membrane vesicles were resuspended in 50 mM KPi, pH 7, plus 3 mM DTT, frozen in liquid nitrogen and stored at -80°C until use. The protein concentration was determined using the DC protein assay (Bio-Rad).

Purification and Immunodetection of LacS-LacS fusion proteins

All steps during the purification were performed at 4°C. *E. coli* MC1061 membrane vesicles (approximately 6 mg total protein) containing LacS fusion proteins were deprived of DTT by washing and subsequently solubilized as described (35). Next, the insoluble fraction was removed by centrifugation (267k x *g*, 15 min) and the supernatant was mixed with 0.25 ml Ni-NTA resin that was washed with ten volumes MilliQ and two volumes of elution buffer (200 mM imidazole (pH 7.0), 10% glycerol) and pre-equilibrated with four volumes of solubilization buffer [15 mM imidazole (pH 8.0), 100 mM NaCl, 10% (v/v) glycerol] supplemented with 0.05% (wt/vol) DDM. The mixture was incubated for one hour with continuous mixing. After that, the column was drained, washed with 30 volumes of solubilization buffer plus 0.05% DDM and eluted with elution buffer plus 0.05% DDM.
Samples were analysed by SDS-PAGE, semi-dry electroblotting and subsequent immunodetection with a primary antibody directed against a hexa-His-tag (Amersham Pharmacia Biotech) as described (35).

Results

A covalent dimer to study subunit interactions

Functional interactions between subunits in dimeric proteins have been studied by mixing active and inactive species in different ratios and characterizing the resulting heterodimers (7,103,119,124), which constitute at most 50% of all dimers, that is, at equal ratio of both species as shown in Fig. 1A (solid line). If the association is random, each of the homodimers makes up 25% at equal ratio of both species. If two species do not interact or function independently, the total activity is determined only by the percentage of active species and will decrease linearly (Fig. 1B, dotted line). However, if both species do interact functionally and the phenotype of one of the species dominates the activity of the heterodimer, the activity will follow a quadratic relationship as shown in Fig. 1B (solid lines); lines *a* and *b* are obtained when a subunit has a negative- or positive-dominant effect on the opposing subunit, respectively.
To determine if the subunits function in a cooperative manner, the specific activity of the heterodimer needs to be resolved. When the exact ratio of the two species is known (e.g., in a proteoliposomal system) this can be determined from the summed activity of all species. However, in whole cells, the ratio of two separately expressed subunits is difficult to control, because of variations in the expression and inaccuracies in the determination of protein levels from, for instance, immunoblots. By covalent coupling of subunits the ratio is known on forehand, which has the additional advantage that the maximum percentage of heterodimers can be elevated from 50% to 100% (see Fig. 1A). This increases the signal that discriminates between independent functioning and negative- or positive-dominant effects of subunits as shown in Fig. 1B.
In order to control the total amount of protein in a reproducible way, expression of the covalent dimer in *E. coli* MC1061 was governed by the arabinose inducible P_{BAD} promoter, which

proved to be a more convenient and reliable expression system than the vector wherein LacS expression was controlled by its endogenous promoter (unpublished data).

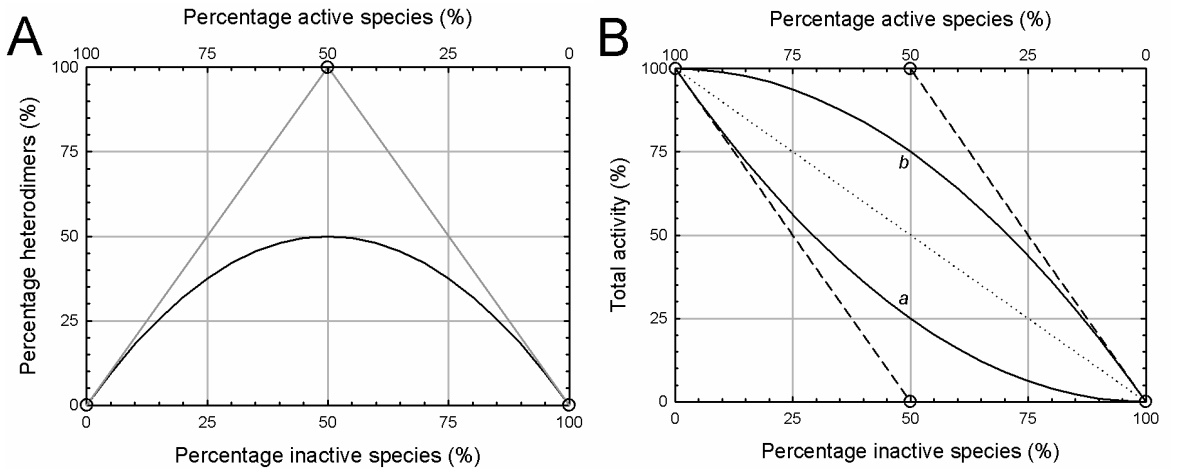

Figure 1. **Comparison between the calculated amount of heterodimers and total activity for free and forced association of two species.** A. The black line depicts the percentage of heterodimers formed as a function of different ratios of active over inactive species, assuming random association. The circles connected by the gray line show the percentage of heterodimers if the subunits are covalently linked. B. The summed activity of all species as a function of different ratios of active over inactive species. The dotted line represents the activity observed if the subunits function independently. Functional dominance of one type of subunit will lead to the solid curves *a* and *b*, representing negative and postive dominance, respectively. Upon fusion of both subunits, these scenarios are represented by the circles connected by the dashed lines. Note that for the forced association of the subunits only three and no intermediate situations exist.

Construction and functional expression of a covalent LacSΔIIA$_2$ dimer

The minimal unit of LacS able to catalyze substrate translocation is the membrane-embedded carrier domain (chapter 3 and (83)). To study the functional interactions of the carrier domains in a defined manner, the covalent LacS dimer comprised two joined LacSΔIIA subunits rather than two LacS subunits. LacSΔIIA lacks the C-terminal LacS-IIA domain that can be phosphorylated by HPr(His~P) (41,83), but shows equal rates of proton-motive-force (Δp)-driven lactose transport and lactose counterflow as unphosphorylated full-length LacS (chapter 3).

Twenty-eight amino acids follow the predicted end of TMS 12 of the first LacSΔIIA(C320A) subunit. An artificial sequence of 15 amino acids was used to link the two subunits. At the DNA level, the linker region contains four endonuclease restriction sites and a sequence coding for a TEV-protease recognition site, yielding the protein sequence GSGDQENLYFQGTSA. Together with the 18 amino acids preceding the predicted start of the first TMS of the second LacSΔIIA(C320A) subunit, the total linker region connecting both subunits comprises 61 amino acids (Fig. 2). This covalent dimer, in which both subunits contain the C320A mutation, was designated LacSΔIIA$_2$(CC).

As shown in Fig. 3, LacSΔIIA$_2$(CC) catalyzed Δp-driven lactose uptake in whole *E. coli* MC1061 cells, demonstrating its functional expression and membrane insertion. Maximal transport activity of LacSΔIIA$_2$ was observed when cells were induced with 2 x 10^{-3}% (wt/vol) L-arabinose, whereas induction with 1 x 10^{-3}% (wt/vol) L-arabinose yielded maximal transport activity of LacSΔIIA (results not shown). At these optimal inducer concentrations, the initial

rates of Δp-driven lactose uptake for LacSΔIIA$_2$(CC) and LacSΔIIA(C320A) were 2.6 and 11 nmol lactose/mg protein*min, respectively. Analysis of the levels of LacSΔIIA$_2$(CC) and LacSΔIIA(C320A) showed that the former was indeed expressed several-fold lower (data not shown).

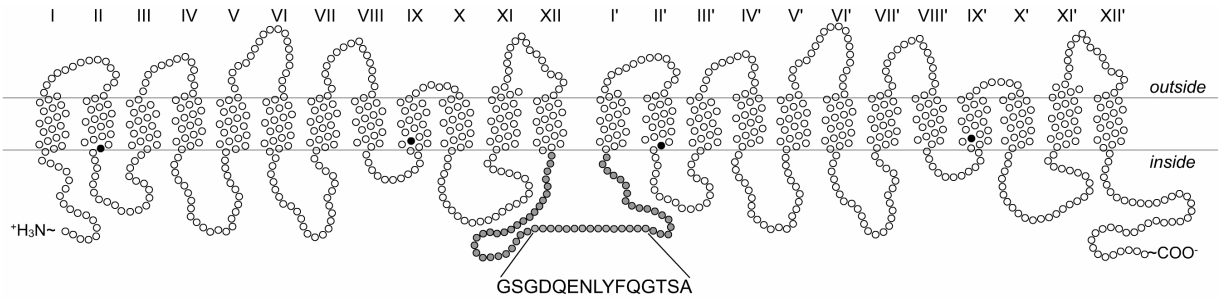

Figure 2. **Topology model of the LacSΔIIA$_2$ dimer.** Membrane topology of the LacSΔIIA subunits is based on the model of MelB (90). The gray horizontal lines indicate the membrane interfaces. Asp-71 in the second transmembrane segment (TMS) of each subunit is depicted in black. The LacSΔIIA subunits are coupled via a linker of 61 amino acids (grey circles). The sequence of the artificially introduced stretch of 15 residues in the linker is shown. In all subunits, the endogenous Cys-320 in TMS IX (also shown in black) was replaced by an alanine residue.

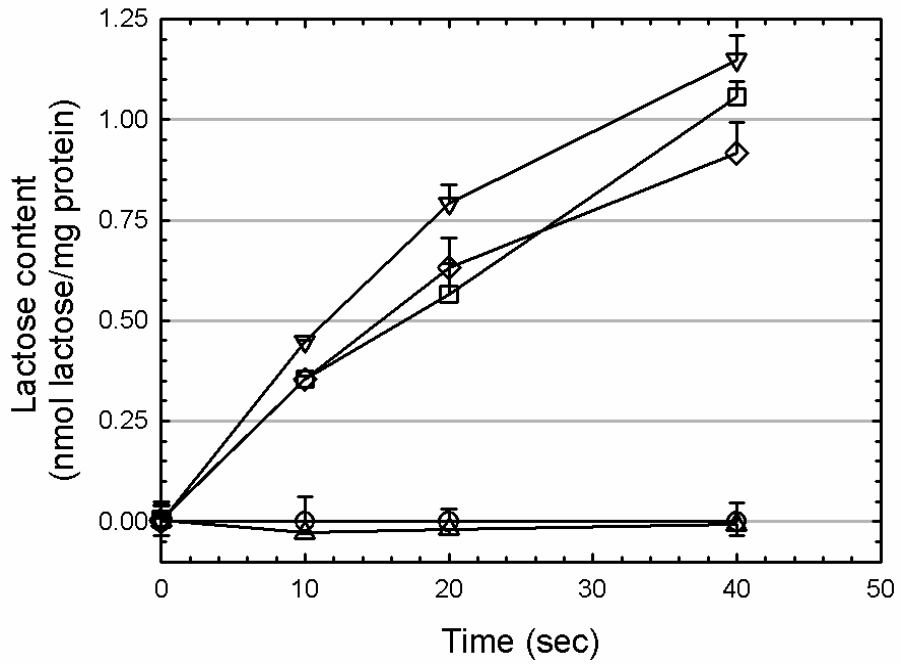

Figure 3. **Δp-driven lactose transport by LacSΔIIA$_2$ derivatives in *E. coli* MC1061.** The accumulation of lactose driven by the proton-motive-force was measured in duplo for LacSΔIIA$_2$(CC) (triangles downwards), LacSΔIIA$_2$(CD) (squares), LacSΔIIA$_2$(DC) (diamonds), LacSΔIIA$_2$(DD) (triangles upwards), and MC1061 cells containing an empty plasmid with an ampicillin resistance marker [pBluescript IISK+ (Stratagene)] (circles).

Inactive D71C/C320A subunits are complemented by active C320A subunits within LacSΔIIA$_2$ during Δp-driven and counterflow transport

Heterodimeric LacSΔIIA$_2$ derivatives were constructed, comprising the D71C mutation in either the first or the second subunit and using the C320A background. The D71C mutation renders

LacS inactive in all modes of transport, but does not affect the overall structure of the transporter as the capacity of LacS(D71C/C320A) to bind substrate was retained (122). The LacSΔIIA$_2$ derivatives containing the D71C/C320A mutation in the first, last, or both subunits were designated LacSΔIIA$_2$(DC), LacSΔIIA$_2$(CD), and LacSΔIIA$_2$(DD), respectively. The mutant variants of LacSΔIIA$_2$ were expressed to comparable levels (Fig. 4A), enabling a direct comparison of the transport activities.

Like the strain containing a control plasmid, cells expressing LacSΔIIA$_2$(DD) showed no significant uptake of lactose in whole *E. coli* MC1061 cells (Fig. 3). The transport rates of LacSΔIIA$_2$(CD) and LacSΔIIA$_2$(DC) were equal, indicating that both halves of the forced dimer are correctly inserted in the membrane. The observed rates of Δp-driven lactose uptake of LacSΔIIA$_2$(CD) and LacSΔIIA$_2$(DC) were approximately 80% of the initial rate of uptake of LacSΔIIA$_2$(CC) (Fig. 3 and 5). This result suggests that the D71C/C320A subunit is partially complemented by the active C320A subunit.

Lactose counterflow transport by the LacSΔIIA$_2$ derivatives showed a similar profile as observed for Δp-driven lactose uptake (Fig. 5). LacSΔIIA$_2$(DD) was completely defective in transport, and both LacSΔIIA$_2$(CD) and LacSΔIIA$_2$(DC) showed approximately 80% of the initial rate of lactose counterflow by LacSΔIIA$_2$(CC), indicating that also for counterflow transport the D71C/C320A subunit is partially complemented by the active C320A subunit.

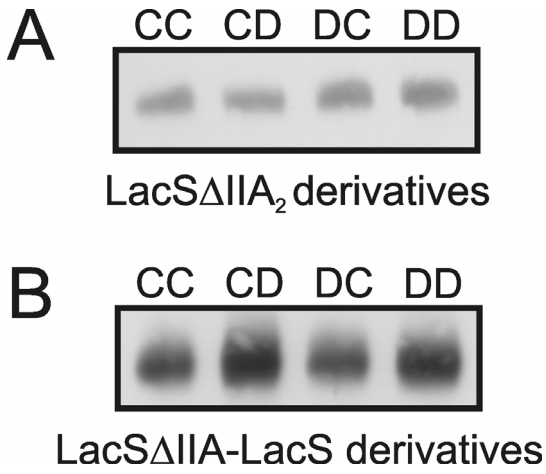

Figure 4. **Immunoblots of covalently-linked LacS derivatives.** LacS derivatives were detected with an antibody directed against a hexa-His-tag. A. Immunoblots of LacSΔIIA$_2$ derivatives, purified from equal amounts of cells. CC and DD represent homodimers of C320A or D71C/C320A subunits, respectively. CD and DC represent heterodimers with a D71C/C320A subunit in the second or first subunit, respectively. B. Immunoblots of the LacSΔIIA-LacS derivatives, purified from equal amounts of cells. The same notation as used in panel A indicates the different LacSΔIIA-LacS derivatives.

Covalent fusion of LacSΔIIA subunits differently affects counterflow and Δp-driven lactose transport

Under identical experimental conditions, non-covalently linked LacS(C320A) showed approximately half the rate of Δp-driven transport compared to lactose counterflow (9.0 and 20 nmol lactose/mg protein*min, respectively), while LacSΔIIA(C320A) showed comparable rates for both modes of transport (11 and 8.6 nmol lactose/mg protein*min). This is most probably caused by a stimulation of the counterflow reaction of LacS(C320A) by HPr(His~P) mediated phosphorylation of LacS-IIA (chapter 3).

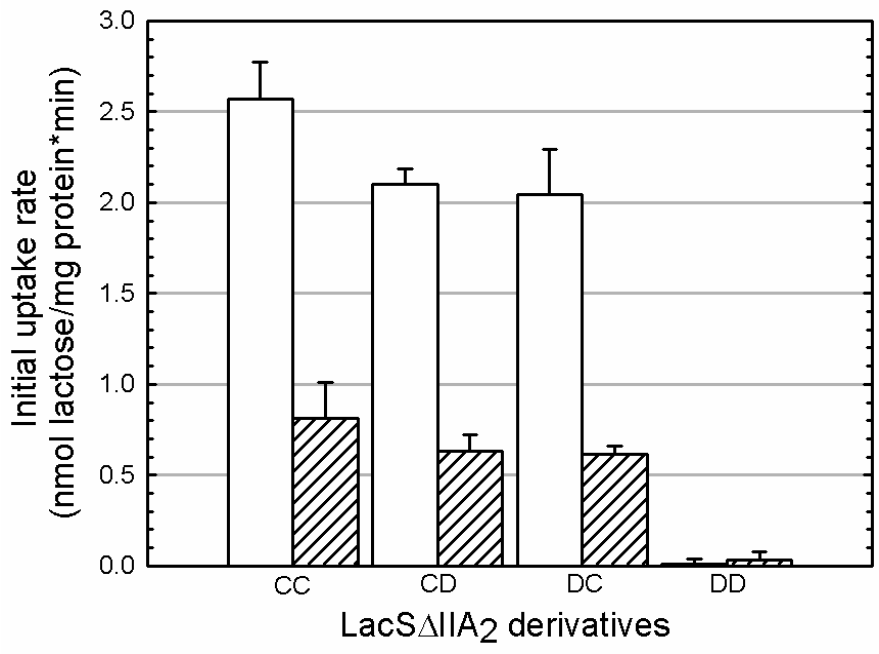

Figure 5. **Initial rates of Δp-driven lactose uptake and lactose counterflow by LacSΔIIA$_2$ derivatives in *E. coli* MC1061.** Counterflow and Δp-driven lactose transport rates were measured on cell suspensions derived from the same culture. To measure lactose counterflow transport, de-energized cell suspensions were preloaded with 10 mM lactose and diluted into buffer containing 100 μM ^{14}C-lactose. Cells used to measure lactose transport driven by the Δp were pre-energized for 2 minutes by incubation with 10 mM D-Li-lactate and aeration. Subsequently, lactose accumulation was started by the addition of 50 μM ^{14}C-lactose. Each rate reflects the average from two independent experiments. Blank and hatched bars reflect initial lactose uptake rates for Δp-driven and lactose counterflow transport, respectively.

Whereas the ratio of the initial rates of Δp-driven transport over counterflow was 0.5 and 1.3 for LacS and LacSΔIIA, respectively, this ratio was approximately 3 for the CC, CD and DC derivatives of LacSΔIIA$_2$ (summarized in Table 2). Since the initial rates of both Δp-driven and counterflow lactose transport were determined on cells derived from the same culture, the discrepancy in relative activities cannot be caused by variation in expression levels. Effects of variations in internal pH between both transport modes on LacSΔIIA$_2$ derivatives could be excluded, because the pH of the buffer during lactose counterflow transport was adjusted to 7.7, which was equal to the internal pH of cells during Δp-driven transport (9). Furthermore, by charging the cells with ^{14}C-lactose, it was shown that the MC1061 cells containing LacSΔIIA$_2$ were equilibrated with lactose to similar levels as those containing non-covalently linked LacSΔIIA(C320A), ruling out limiting intracellular lactose concentrations as a cause for the decreased counterflow transport rates. We therefore conclude that the 3-fold difference in initial rates of Δp-driven lactose transport and lactose counterflow transport by the CC, CD, and DC derivatives of LacSΔIIA$_2$ is a genuine property of these dimers.

A more detailed kinetic analysis of lactose exchange transport, which comprises the same kinetics steps as counterflow transport and only differs from counterflow in substrate concentrations and the location of the carbon-14 isotope of lactose (inside for exchange, outside for counterflow), was conducted (Fig. 6). All LacSΔIIA$_2$ derivatives showed similar lactose exchange kinetics, again reflecting that all subunits (irrespective of the order of active C320A and inactive D71C/C320A subunits) were affected equally by the covalent linkage. Moreover, the apparent affinity constants of the LacSΔIIA$_2$ derivatives for lactose were

maximally only two-fold increased compared to the K_m^{App} of LacSΔIIA, suggesting that the overall structure of both subunits in the LacSΔIIA$_2$ derivatives is conserved. Summarizing, it seems that both subunits within the LacSΔIIA$_2$ derivatives adopt a correct conformation.

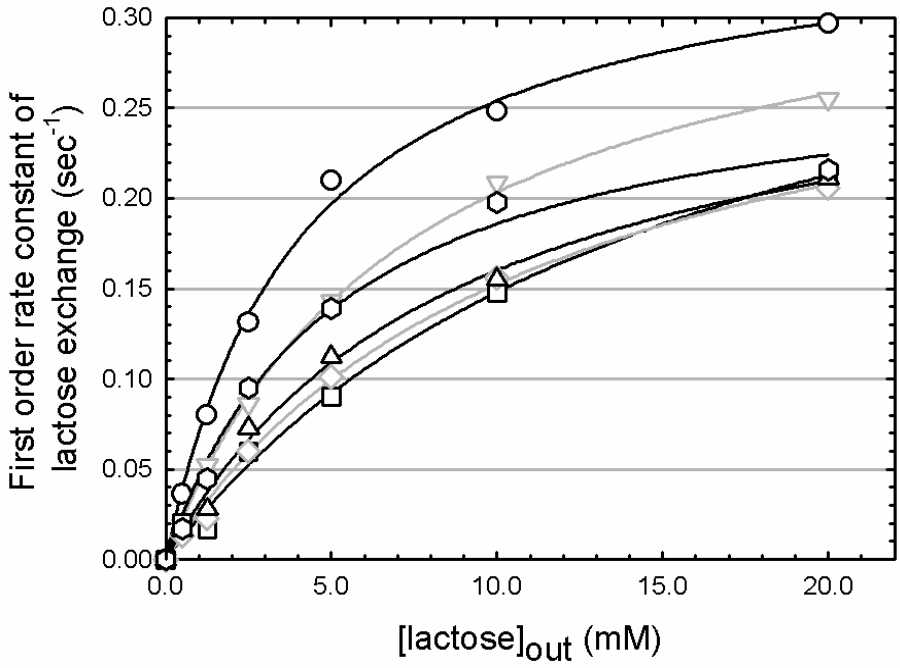

Figure 6. **Kinetics of lactose exchange transport by LacS derivatives in *E. coli* MC1061.** The initial rates of lactose exchange was measured for LacS (circles), LacSΔIIA (triangles downwards), LacSΔIIA$_2$(CC) (squares), LacSΔIIA$_2$(CD) (diamonds), LacSΔIIA$_2$(DC) (triangles upwards), and LacSΔIIA-LacS(CC) (hexagonals). Concentrated, de-energized cell suspensions were charged overnight with 5 mM ^{14}C-lactose and the transport reaction was initiated by 100-fold dilution of the cells into KPM pH 7.7, supplemented with 50 μM SF6847. The external lactose concentration varied from 50 μM to 20 mM. To enable accurate determination of the kinetics of lactose exchange transport, cells expressing LacS or LacSΔIIA were induced by a 7-fold lower L-arabinose concentration than used for counterflow and Δp-driven lactose transport. The exit of ^{14}C-lactose from the cells was mono-exponential and the half-time of the decay was used to calculate the first order rate constant (k_{ex}). The k_{ex} was plotted against the external lactose concentration and fitted with the Michaelis-Menten equation.

The LacS-IIA domain primarily interacts with the subunit of LacSΔIIA-LacS to which it is attached

Upon HPr(His~P) mediated phosphorylation of His-552 in the LacS-IIA domain, the LacS-IIA domain interacts with the carrier and thereby stimulates lactose counterflow (chapter 3 and (41)). To determine whether the regulation of the LacS-IIA domain occurs inter- or intramolecularly, a tandem fusion was constructed in which the last subunit has a C-terminal LacS-IIA domain attached to the carrier domain, creating a topology equal to the full-length LacS protein. This construct was designated LacSΔIIA-LacS. The mutant variants derived from this construct, harbouring the D71C mutation, were not expressed to an equal level as shown in Fig. 4B. Constructs containing the D71C substitution in the second subunit were expressed to a higher level than subunits without a D71C mutation. This variation in expression levels only allowed a qualitative analysis, since exact quantification of the amount of functional transporters was at this stage not possible due to the lack of a suitable ligand binding assay.

The rate of Δp-driven lactose uptake of LacSΔIIA-LacS(CC) was in the same range as the rate of LacSΔIIA$_2$(CC) (2.8 and 2.6 nmol lactose/mg protein*min, respectively) (Fig. 7).

Furthermore, the kinetics of lactose exchange by LacSΔIIA-LacS(CC) yielded an apparent affinity constant for lactose similar to that of the other LacS derivatives (Fig. 6). In line with the observations on the LacSΔIIA$_2$ derivatives, both LacSΔIIA-LacS(CD) and LacSΔIIA-LacS(DC) were active in Δp-driven transport, whereas LacSΔIIA-LacS(DD) was inactive (Fig. 7).

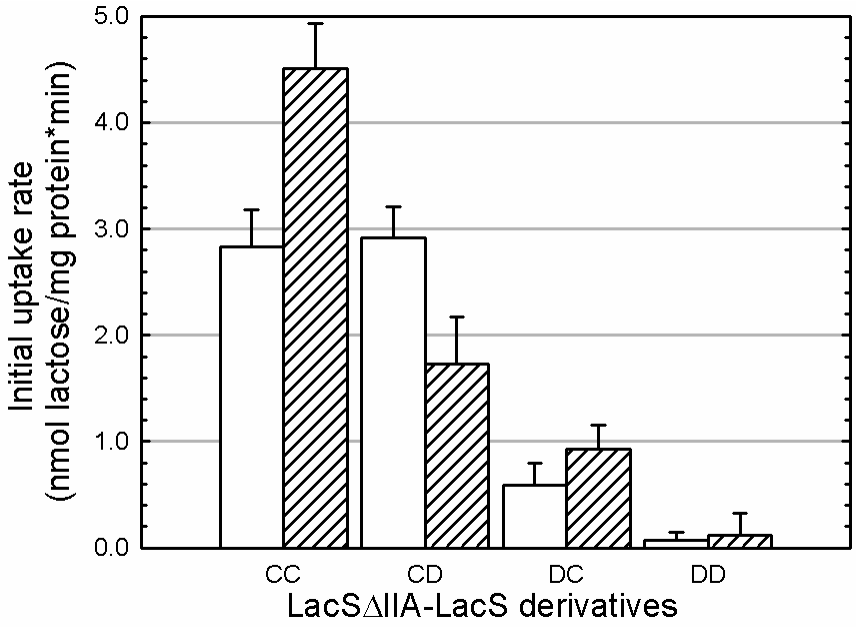

Figure 7. **Initial rates of Δp-driven lactose uptake and lactose counterflow by LacSΔIIA-LacS derivatives in *E. coli* MC1061.** Counterflow and Δp-driven lactose transport rates were measured on concentrated cell suspensions derived from the same culture as described in the legend of Fig. 5. Each rate reflects the average from two independent experiments. Blank and hatched bars reflect initial lactose uptake rates for Δp-driven and lactose counterflow transport, respectively.

As described heretofore, the ratio of the initial rates of Δp-driven transport over counterflow was 0.5 and 1.3 for LacS and LacSΔIIA, respectively, while this ratio was close to 3 for the CC, CD and DC derivatives of LacSΔIIA$_2$ (summarized in Table 2). Both LacSΔIIA-LacS derivatives that had a LacS-IIA domain attached to the active C320A subunit (LacSΔIIA-LacS(CC) and LacSΔIIA-LacS(DC)) showed a ratio of Δp-driven transport over counterflow of approximately 0.6. In contrast, for LacSΔIIA-LacS(CD), this ratio was elevated to 1.7. Since the ratio differs for the LacSΔIIA-LacS(CD) and LacSΔIIA-LacS(DC) constructs, this strongly suggests that the IIA domain is restricted in its opportunity to interact with the carrier domains within the LacS dimer. Most likely, it cannot interact with any nearby subunit but only with the subunit to which it is attached.

Discussion.

Several independent studies led to the conclusion that the detergent-solubilized LacS protein is in monomer to dimer equilibrium (32,35,48), whereas membrane-embedded LacS is dimeric (32,35,109). Veenhoff et al. (124) showed by *in vitro* analysis of membrane-reconstituted (conditionally) inactive LacS(E67C/C320A) and active LacS(C320A) species that, within this structural dimer, functional interactions between the subunits take place in Δp-driven uptake but not in counterflow transport. Here, we report the first *in vivo* demonstration of functional interactions between the subunits within the LacS dimer and show that both subunits functionally interact not only in Δp-driven transport but also in counterflow. We show that (*i*) the

activity of the D71C mutant is (partially) restored by an active subunit; (*ii*) covalent linkage of two LacS subunits increases the rate of ∆p-driven uptake relative to counterflow transport; and (*iii*) phosphorylation of the LacS-IIA domain stimulates the *cis* rather than the *trans* subunit of dimeric LacS.

Due to its uncoupled phenotype in whole cells, resulting in rapid efflux of lactose down the concentration gradient, LacS(E67C/C320A), previously used to demonstrate functional interactions within the LacS dimer *in vitro* (124), could not be used to study subunit interactions in whole cells. Instead, the translocation-defective but lactose binding-competent LacS(D71C/C320A) was employed. Both Glu-67 and Asp-71 are located in TMS II and acidic residues at these positions are highly conserved throughout the GPH-family. Glu-67 has been proposed to be involved in coupling proton and galactoside transport, whereas Asp-71 is thought to contribute to the proton binding site (84). In addition, both residues are in a region that is conformationally active upon substrate-binding (122). Membrane-reconstituted LacS(E67C/C320A) catalyzes lactose counterflow transport at ~80% of the rate of LacS(C320A) and after modification of Cys-67 with NEM ~30% activity remained. LacS(E67C/C320A) is completely defective in ∆p-driven lactose transport (124). In contrast, LacS(D71C/C320A) is inactive in both ∆p-driven lactose transport and lactose counterflow, but the overall structure of the protein is retained as substrate-binding still occurs. Several second-site suppressor mutations of Cys-71 have been isolated, among which R230C, which could restore lactose counterflow transport but not ∆p-driven lactose transport (122). By employing LacS(D71C/C320A) in tandem constructs with LacS(C320A), the effect of a subunit defective in all transport modes could be determined.

The LacS∆IIA$_2$ derivatives were functionally expressed, although the levels were lower than those of the free subunits, as observed before for other *in tandem* fusion proteins (99,119). The expression levels of the different LacS∆IIA$_2$ derivatives were equal based on immunoblotting (Fig. 4A), but this technique lacks the sensitivity to demonstrate small variations (<20%) in expression levels. The LacS∆IIA$_2$(CC) was functional in both ∆p-driven and lactose counterflow transport and both subunits are membrane-inserted as LacS∆IIA$_2$(CD) and LacS∆IIA$_2$(DC) showed similar transport rates. LacS∆IIA$_2$(DD), which resembles the LacS(D71C/C320A) homodimer, is inactive, indicating that the mere coupling of the subunits is not sufficient for the restoration of the transport capacity. The difference in the ratio between the initial rates of ∆p-driven lactose transport and lactose counterflow for the LacS∆IIA$_2$ derivatives when compared with LacS∆IIA and LacS, suggest that either ∆p-driven lactose transport benefits or lactose counterflow activity deficits from the fusion of the subunits (Table 2). Kinetic analysis of lactose exchange transport showed that substrate-binding of the LacS∆IIA$_2$ derivatives was only slightly affected, because the K_m^{App} was at most two-fold higher than the K_m^{App} of the LacS∆IIA dimer. Taken together, the covalent coupling of subunits only introduces some moderate changes within the LacS dimer and seems a valid system to study subunit interactions.

For independent operating subunits within the LacS dimer, the heterodimers LacS∆IIA$_2$(CD) and LacS∆IIA$_2$(DC) would be expected to show half the initial transport rates of LacS∆IIA$_2$(CC). A negative dominant phenotype of the D71C subunit would yield inactive LacS∆IIA$_2$(CD) and LacS∆IIA$_2$(DC) heterodimers. Clearly, both scenarios do not apply since the initial rates of LacS∆IIA$_2$(CD) and LacS∆IIA$_2$(DC) for both ∆p-driven lactose transport and lactose counterflow were approximately 80% of the rates of LacS∆IIA$_2$(CC) (Table 2). Rather,

these transport activities support the contention that the C320A subunit has a positive dominant effect, since it is able to partly restore the activity of the LacSΔIIA(D71C/C320A) subunit.

Table 2. **Overview of the topology and transport rates of the LacS derivatives.** The LacSΔIIA(C320A) and LacSΔIIA(D71C/C320A) subunit are presented as a rectangle, and a rectangle filled with a cross, respectively. The LacS-IIA domain is depicted as a flattened sphere. The initial transport rates were determined as described in the legend of Fig. 5.

LacS derivative	Topology	Initial transport rate (nmol lactose/mg protein*min)		Ratio Δp-driven / counterflow
		Δp-driven	counterflow	
LacS(C320A)		9.04 ± 1.77	20.31 ± 0.53	0.45
LacSΔIIA(C320A)		11.14 ± 0.59	8.59 ± 0.75	1.30
LacSΔIIA$_2$(CC)		2.57 ± 0.21 (100%)	0.81 ± 0.20 (100%)	3.17
LacSΔIIA$_2$(CD)		2.10 ± 0.08 (82%)	0.63 ± 0.09 (78%)	3.33
LacSΔIIA$_2$(DC)		2.04 ± 0.25 (79%)	0.61 ± 0.05 (75%)	3.34
LacSΔIIA$_2$(DD)		0.01 ± 0.03 (0%)	0.03 ± 0.04 (4%)	X
LacSΔIIA-LacS(CC)	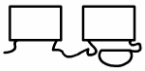	2.83 ± 0.35	4.51 ± 0.42	0.63
LacSΔIIA-LacS(CD)		2.92 ± 0.29	1.73 ± 0.44	1.69
LacSΔIIA-LacS(DC)		0.59 ± 0.21	0.93 ± 0.22	0.63
LacSΔIIA-LacS(DD)		0.07 ± 0.08	0.11 ± 0.21	X

Our new findings differ in some aspects from previous observations, using a proteoliposomal system, which demonstrated functional interactions between the LacS subunits for Δp-driven lactose transport only (124). In proteoliposomes, increasing the percentage of impaired LacS(E67C/C320A) over LacS(C320A) resulted in a linear decrease in lactose counterflow transport, suggesting that the subunits function independently during this mode of transport. Furthermore, heterodimers composed of inactive LacS(E67C/C320A) and active LacS(C320A) were shown to be completely inactive in Δp-driven lactose transport, indicating negative dominance of the LacS(E67C/C320A) subunit. In the present study, negative dominance of the LacSΔIIA(D71C/C320A) subunit in LacSΔIIA$_2$(CD) or (DC), is clearly not observed. Rather than interpreting these discrepancies in terms of differences in the experimental context (proteoliposomes *versus* intact cells), we feel that they can be explained by the different phenotypes of the LacS(E67C/C320A) and LacS(D71C/C320A) mutants. Most likely, LacS(D71C/C320A) is locked in one conformation, since it has lost its ability to reorient its substrate-binding sites as required for transport while retaining the ability to bind substrate (122). An opposing functional subunit could enable the LacSΔIIA(D71C/C320A) to overcome

this locked conformation, leading to (partial) complementation. LacS(E67C/C320A), on the other hand, kept the ability to reorient its binding sites and thereby catalyze lactose counterflow transport. Only its ability to catalyze ∆p-driven lactose transport was impaired. As the extent of the impairment is different for both mutants, this may explain the lack of complementation of LacS(E67C/C320A) by LacS(C320A).

Apart from the relative activities of the different LacS∆IIA$_2$ derivatives for either ∆p-driven lactose uptake or lactose counterflow, the ratio of the initial rates of ∆p-driven lactose transport over counterflow reveals interesting features. This ratio is approximately 3 for the CC, CD and DC derivatives of LacS∆IIA$_2$, while it is close to 1 for LacS∆IIA. It is likely that the difference in the ratio of the initial rates for LacS∆IIA$_2$ compared to LacS∆IIA is a specific property of the fusion protein, caused by the presence of the linker connecting both subunits. A possible consequence of the covalent coupling could be the decreased ability of the subunits to separate transiently.

Additionally, the mere presence of the LacS-IIA domain to the second subunit decreased the ratio of ∆p-driven transport over counterflow from ~3 to 0.6 – 1.7, indicating that phosphorylation of this domain affects the subunit interactions. Since the absolute rates of ∆p-driven lactose transport of LacS∆IIA$_2$(CC) and LacS∆IIA-LacS(CC) are similar, it seems that the rate of lactose counterflow transport is increased upon addition of the LacS-IIA domain. Therefore, it is tempting to speculate that the kinetic step that is impaired by the coupling of the subunits is the same as the one that is stimulated by the phosphorylation of the LacS-IIA domain. Thus, the phosphorylated LacS-IIA domain could induce a transient conformation of the carrier domain that is less strongly interacting with the opposing subunit.

Under the conditions used, the IIA-domain of LacS is phosphorylated in *E. coli* MC1061, resulting in an increase in the rate of counterflow transport and a decrease in the ratio of ∆p-driven transport over counterflow (chapter 3). Phosphorylation of the LacS-IIA domain in the LacS∆IIA-LacS derivatives resulted in a ratio of ∆p-driven transport over counterflow near 0.6 if the LacS-IIA domain was associated with the LacS∆IIA(C320A) subunit (Fig. 7), and near 1.7 if it was associated with the inactive D71C subunit. The difference in the ratio of both transport modes observed for LacS∆IIA-LacS(CD) and LacS∆IIA-LacS(DC) suggests that the LacS-IIA domain prefers to functionally interact with the subunit to which it is attached. Although the rate of lactose counterflow is relatively increased for LacS∆IIA-LacS(CD), the increase is smaller than that observed for the CC and DC derivatives of LacS∆IIA-LacS, indicating that the D71C/C320A subunit cannot be stimulated by phosphorylated LacS-IIA to the same extent as the C320A subunit.

Taken together, the data presented here strengthen the conclusion that the two subunits of the LacS dimer functionally interact, not only *in vitro* as separate proteins but also *in vivo* in tandem fusions. The functional interactions within the LacS dimer take place during both ∆p-driven lactose transport and lactose counterflow and can be both positive and negative of nature. Furthermore, the LacS-IIA domain primarily stimulates transport through intramolecular interactions with the carrier domain.

Acknowledgements

E.R.G. acknowledges J.H.A. Folgering and L.M. Veenhoff for helpful discussions and the EU-FP6 programme (E-Mep; 504601) for funding.